Original article

Effect of indomethacin on embryo implantation and histomorphology of uterus, ovary, kidney, and liver of rats

Maria Amir [a,c], Nurhusien Yimer [a,b,*], Mark Hiew [a], Sabri Mohd Yusoff [e], Bedru Hussen [f], Abdul Quddus [d]

[a] Department of Veterinary Clinical Studies, Faculty of Veterinary Medicine, Universiti Putra Malaysia, 43400 Serdang, Selangor, Malaysia
[b] Department of Veterinary Reproduction, Faculty of Veterinary Medicine, Universitas Airlangga, 60115 Surabaya, East Java, Indonesia
[c] Faculty of Veterinary and Animal Sciences, Department of Veterinary Physiology and Biochemistry, Ziauddin University, 75600 Karachi, Pakistan
[d] Faculty of Veterinary and Animal Science, Lasbela University of Agriculture Water and Marine Science, 90150 Uthal, Balochistan, Pakistan
[e] Department of Veterinary Pathology and Microbiology, Faculty of Veterinary Medicine, Universiti Putra Malaysia, 43400 Serdang, Selangor, Malaysia
[f] School of Public Health, University of Hong Kong, 7 Sassoon Rd, Sandy Bay, Hong Kong

ARTICLE INFO

ABSTRACT

Background: This study aimed to determine the effects of Indomethacin (IMC) treatment on embryo implantation and histomorphology of uterus, ovary, and other vital organs and its effective dosage in establishing embryo implantation dysfunction model in Sprague-Dawley (SD) rats.

Materials and Methods: The experiments were performed on 24 (6 × 4 groups) adult female SD rats aged 12 weeks old. G1 was the control group and received a normal diet with normal saline. However, on pregnancy days 3 (Pd3) and 4 (Pd4), G2, G3, and G4 were given normal saline and subcutaneously administered IMC twice daily at different doses of 4.33, 4.66 and 5.00 mg/kg body weight, respectively. The rats were euthanized on day 8 of pregnancy (Pd8). The uterus was excised and examined for signs of pregnancy, followed by tissue samples from liver, kidney, and ovary (for histomorphological examination using haematoxylin and eosin stain).

Results: All IMC treatment doses disrupted the implantation process and caused a significant reduction in embryo development. Analysis for histopathological changes revealed that IMC doses above 4.33 mg/kg body weight caused more adverse reproductive health effects in rats. Vasoconstriction and micro vascularization were detected in the liver, while degenerative Bowman's capsules and inflammatory cells were observed in kidney sections from IMC-treated rats.

Conclusion: IMC therapy interfered with implantation and embryo development in rats, resulting in significant uterine vasoconstriction and atrophy, 4.33 mg/kg bwt dose appeared to be optimum to establish embryo implantation dysfunction in SD rats.

1. Introduction

In mammals, implantation occurs through a successful interaction between implantable blastocyst and endometrium. Both molecular and cellular activities remain imperative for embryo implantation, as well as the essential processes required for implantation (Andrabi & Maxwell, 2007; Lü et al., 2019). An adequate dosage can be ascertained to establish embryo implantation dysfunction (EID) without severely affecting other vital organs of the body, i.e., the synchronized preimplantation (PIP) embryo development and uterine differentiation (UD)

to the receptive state (Tranguch et al., 2005). Ovulation and implantation are also processes that resemble pro-inflammatory reactions (Cavalieri et al., 1998). PGE2 and PGF2 alpha play critical roles in endometrial vascular permeability, leukocyte recruitment during implantation, stromal decidualization, and, most importantly, blastocyst growth and development (Fu et al., 2020; Olivera-Muzante et al., 2019). COX-derived PGs are vital for successful implantation (Andrabi & Maxwell, 2007; Salleh, 2014). However, these roles of PG in the uterus can be affected by (non-steroidal anti-inflammatory drugs) NSAIDs such as IMC through inhibition of PG synthesis.

IMC is very effective in treating inflammation in animals. Rodents have a receptive uterus and a 4–5-day estrous cycle (Thompson et al., 2020). A columnar epithelium and stromal cells make up its uterine endometrium. After ingestion of IMC, the NSAID inhibits the COX enzyme, which exists in two isoforms: COX-1 and COX-2. COX-1 is expressed in the uterine luminal and glandular epithelial cells in the morning of Pd4 (Poyser, 1999) but is almost undetectable during the attachment response. COX-2 is only expressed in the luminal epithelium beneath the stromal cells and is essential for implantation during the attachment reaction (Thompson et al., 2020).

Prostaglandins play an important role in ovulation. In particular, prostaglandin E2 (PGE2) and prostaglandin F2α (PGF2α) concentrations increase massively prior to ovulation (Vernunft et al., 2022). In addition to limiting prostaglandin production and preventing follicular rupture with oocyte release (Yavuz et al., 2021). It has been shown that IMC, when administered before ovulation, prevents follicle rupture without apparent effects on serum Follicule stimulating hormone (FSH), Luteinizing hormone (LH), estradiol and progesterone concentrations (Duncan, 2019). Prostaglandins inhibitor IMC synergistically blocks ovulation (Yerushalmi et al., 2023), injection of IMC into single follicle inhibit the release of these follciles (Yerushalmi et al., 2023).

IMC causes multisystem lesions in a variety of tissues, including the kidney, liver, stomach, brain, lungs, blood vessels, and glands, in different experimental animal species, leading to deterioration, necrosis, and erosion (Sathyanarayanan et al., 2022). According to morphological studies, IMC caused the kidney's ultrastructure to change, resulting in papillary necrosis, acute renal failure, tubular degeneration, nephritic syndrome with interstitial nephropathy, increased mitochondria, and papillary necrosis (Steenbergen et al., 2020). The use of IMC by the pregnant mother also indicated a potential contributor to renal dysfunction, including glomerular damage, renal insufficiency, and caused death in newborn infant due to renal failure (Khan et al., 2019). IMC and other NSAIDS have also been linked to wide-spread necrosis, particularly in the stomach, ulcers in the small intestine, DNA damage, mitochondrial damage, and coagulative necrosis of the liver (Mahmoud et al., 2023; Parthasarathy & Evan Prince, 2021).

There has been little research on the efficiency of IMC therapy in creating EID in SD rats. This experiment was carried out to analyse usage of IMC to establish embryo implantation malfunction in SD rats by assessing embryo development as well as histomorphological abnormalities in uterine, ovary, liver, and kidney tissues. The current study assessed embryo development and histo-morphological changes in uterine, ovarian, liver, and kidney tissues in SD rats.

2. Materials and Methods

2.1. Ethical approval

The Institutional Animal Care and Use Committee at Universiti Putra Malaysia (UPM) approved all studies (Project approval number: UPM/IAUC/AUR09/2016).

2.2. Preparation of IMC and its dosage

A commercially available IMC (Methacid) in tablet form (Sunward Pharma Company, Malaysia) (25 mg each) stored at 25–30 °C was used in the study. 1 g of IMC powder in 100 ml distilled water made a stock solution. This solution was then cooled to 4 °C. At Pd3 and Pd4, each treatment group (G2, G3, G4) received IMC doses of 4.33, 4.66, and 5.00 mg/btw twice daily (at 9 am and 4 pm). The control group (G1) received the same volume of normal saline (Table 1).

2.3. Experimental design

The experiments were performed on 24 (6 × 4 groups) adult female Sprague-Dawley rats (SD rats) aged 12 weeks old (A-Sapphire Animal

Table 1
Animal grouping and treatment regime.

Group	Assignment (6 rats/group)	Type of feed (dose)/2 weeks
Control Treatment Group	G1 (Control)	Normal diet + Normal saline
	G2 (Low dose)	Normal diet + IMC (4.33 mg/kg bwt.)
	G3 (Medium dose)	Normal diet + IMC (4.66 mg/kg bwt.)
	G4 (High dose)	Normal diet + IMC (5.00 mg/kg bwt.)

[1]Body weight (bwt). *G1 = Control, G2 = IMC (4.33 mg/kg bwt), G3 = IMC (4.66 mg/kg bwt) and G4 = (IMC 5.00 mg/kg bwt).

Resource Centre, Selangor, Malaysia). All the rats were housed in a controlled environment with a room temperature of 22 ± 3 °C. After seven days of acclimatization, the rats were randomized into 4 (6 animals/group) and subjected to in vivo supplementation of IMC according to Table 1 below for a period of 2 weeks.

2.4. Tissue sampling, staining and evaluation under a microscope

Under general anaesthetic, the rats were sacrificed on Pd8. The Histopathology Laboratory at the Universiti Putra Malaysia (UPM) Faculty of Veterinary Medicine processed the organ samples. The ovary, uterine, kidney, and liver tissues were excised. The gross examinations were noted, the observable anomalies were rinsed with normal saline, and the 10 % neutral buffered formalin was used to fix them. Under general anaesthesia, the rats were sacrificed on the Pd8. Processed the organ samples at the Histopathology Laboratory, Faculty of Veterinary Medicine, Universiti Putra Malaysia (UPM). Tissue samples from the ovary, uterus, kidney, and liver were excised, examined, washed with normal saline, and fixed using 10 % neutral buffered formalin. A rotary cutting microtome (Leica Biosystems, Nussloch, Germany) was used to trim samples approximately 3 ~ 5 μm thick. The uterine, ovarian, liver, kidney tissue samples were examined microscopically to determine histological changes. The tissues were quantified through observation at x400 magnification in 10 fields of 6 different sections obtained from 3 rats per group. The average number of cells, for the ten fields were computed and calculated for each section and analyzed with Graph pad prism (Panzan et al., 2013). In addition, the number of ovarian follicles and interstitial cells was examined and analyzed using Medical Image Analysis software. The antral space, cell shape, and number of layers surrounding the oocyte were used to categorise these follicles. Primordial, primary, secondary, tertiary or antral, and atretic follicles were the different types of follicles classified in accordance with the presence of antral space and the number of cell layers surrounding the egg (Luo et al., 2008). Quantification of the interstitial cells was performed at 400 × magnification in ten non-overlapping fields from six different sections obtained from three animals from each group (Abubakar et al., 2019; Quddus et al., 2021). Uterine tissue samples were harvested, cleared of any connective 90 tissue, and weighed using an electronic weighing balance. Any visible abnormalities found during the gross examinations were noted. We also studied and graded toxicological abnormalities in the liver, including inflammation, activated kupffer cells, hydropic degeneration, regeneration, and necrosis. Meanwhile toxicological lesions in the kidney tissue were studied and graded, these included cellular cast, granular cast, protein cast, inflammation, hydropic degeneration, and necrosis. Lesions were graded as 0 (normal), 0.5 (very mild), 1.0 (mild), 1.5 (mild to moderate), 2 (moderate), 2.5 (moderate to severe), and 3.0 (severe) in both liver and kidney tissues. The detail description for lesion scoring method are presented in Tables 2, 3, 4 and 5.

Table 2
Mean scores of histopathological lesions in ovaries of rats exposed to IMC.

Parameters	Ovaries			
	Groups			
	G1	G2	G3	G4
Necrosis in interstitial cells*	0 ± 0[a]	1.33 ± 0.58[a]	1.67 ± 0.58[b]	2.33 ± 1.54[c]
inflammatory cells	0 ± 0[a]	2 ± 0[b]	2 ± 1[c]	2.67 ± 0.58[d]
Congestion	0 ± 0[a]	1.67 ± 0.58[b]	2 ± 1[c]	2.83 ± 0.29[d]

Table 3
Mean scores of histopathological lesions in the uterine tissues of rats exposed to IMC.

Parameters	Uterus			
	Groups			
	G1	G2	G3	G4
Vacuolation*	0 ± 0[a]	1.67 ± 0.58[b]	1.83 ± 0.2[b]	2.33 ± 0.58[c]
Necrosis *	0 ± 0[a]	1.31 ± 0.58[a]	2.33 ± 1.15[c]	1.83 ± 0.41[b]
Infiltration of inflammatory cells	0 ± 0[a]	1.33 ± 0.58[a]	2.33 ± 0.57[c]	2 ± 1[c]
Congestion	0 ± 0[a]	1.33 ± 0.58[a]	1.67 ± 0.57[b]	2.67 ± 0.75[c]

Data are expressed as M ± SEM. Different letters a, b, and c across rows denote a significant difference at p < 0.05. *G1 = control, G2= (4.33 mg/kg bwt), G3= (4.66 mg/kg bwt), G4= (5.00 mg/kg bwt).

Table 4
Mean scores of histopathological lesions in the kidney tissues of rats exposed to IMC.

Parameters	Kidney			
	Groups			
	G1	G2	G3	G4
Vacuolation*	0 ± 0[a]	1 ± 0[a]	1.33 ± 1.53[a]	2 ± 1[c]
Necrosis *	0 ± 0[a]	2 ± 0[b]	2.33 ± 1.55b	2.33 ± 0.58[c]
Infiltration of inflammatory cells	0 ± 0[a]	2 ± 0[b]	2.33 ± 0.58[c]	2 ± 1[c]
Congestion	0 ± 0[a]	1.33 ± 0.58[a]	1.67 ± 0.577[a]	3 ± 0[c]
Atrophy of the glomerulus	0 ± 0[a]	1 ± 0[a]	1.67 ± 0.577[a]	2.67 ± 058[c]

Data are expressed as M ± SEM. Different letters a, b, and c denote a significant difference at p < 0.05. *G1 = control, G2= (4.33 mg/kg bwt), G3= (4.66 mg/kg bwt), G4= (5.00 mg/kg bwt).

Table 5
Mean scores of histopathological lesions in liver tissues when exposed to IMC.

Parameters	Liver			
	Groups			
	G1	G2	G3	G4
Vacuolation*	0 ± 0[a]	1.33 ± 0.58[b]	1.33 ± 1.53[b]	2.17 ± 0.29[c]
Necrosis *	0 ± 0[a]	1.67 ± 0.58[b]	2.33 ± 1.15[b]	2.5 ± 0.5[c]
Infiltration of inflammatory cells	0 ± 0[a]	2.33 ± 1.55[b]	2 ± 0[b]	3 ± 0[c]
Congestion	0 ± 0[a]	1.33 ± 1.53[b]	1.67 ± 0.58[b]	2.67 ± 058[c]
Activation of Kupffer cells	0 ± 0[a]	1.33 ± 0.58[b]	1.67 ± 0.58[b]	2.67 ± 058[c]

Data are expressed as M ± SEM. Different letters a, b, c denote a significant difference at p < 0.05. *G1 = control, G2= (4.33 mg/kg bwt), G3= (4.66 mg/kg bwt), G4= (5.00 mg/kg bwt).

2.5. Estrous cycle determination and synchronization

At the beginning of the experiment, the rats were given two 0.5 mg intraperitoneal doses of estrumate, spaced three days apart (Pallares & Gonzalez-Bulnes, 2009). All animals had vaginal smears taken every morning for four weeks to assess the regularity of their estrous cycles, and cytological analysis using light microscopy was performed according to (Albishtue et al., 2018).

2.6. Statistical analysis methods

The data was analysed using GraphPad Prism 6.0 (GraphPad Software, San Diego, California). The ovarian body weight ratio (OBWR), uterine body weight ratio (UBWR), fertility index, and pregnancy rate were compared using one-way ANOVA with Tukey's multiple comparisons post-hoc analysis. The Mann-Whitney-*U* test, which is non-parametric, was employed to compare the two groups. Using two-way ANOVA with Bonferroni's multiple comparison tests, body weights, ovarian follicle types, and corpus luteum were compared, and p0.05 was regarded as significant.

3. Results

3.1. Oestrous cycle

Fig. 1 shows the representative photomicrographs of the phases of the estrous cycle. It displays the variations in the ratio and type of vaginal cells at different cycle stages. All rats had a normal estrous cycle length (4 days), and three different cell types were observed in the vaginal smears. Groups of round-nucleated epithelial cells with separate, mildly stained cytoplasm and oval nuclei were seen during the pro-oestrous stage (Fig. 1A). During the oestrus stage, packed clusters of cornified squamous epithelial cells were seen (Fig. 1B). Poly-morphonuclear leukocytes and a few cornified epithelial cells were present during the metoestrous stage (Fig. 1C). Less cornified and nucleated epithelial cells and more leukocytes were present during the dioestrous stage (Fig. 1D). After mating, sperm cells were seen during oestrus (Fig. 2). Pd1 was designated upon the detection of sperm in the vaginal smear; this detection is shown in Fig. 2. In Pd3 and Pd4, rats in all groups underwent subcutaneous injections of IMC (4.33, 4.66, and 5.00 mg/kg bwt) twice a day. Ovarian, uterine, liver, and kidney samples were collected for histopathological examination. The fertility index was obtained by dividing the number of pregnant females by the total number of animals that copulated and multiplying the result by 100. The pregnancy rate was calculated by dividing the number of pregnancies at term by the number of females mating.

3.2. Effect of IMC on maternal body weight, OBWR and UBWR

Fig. 3 shows the average body weight of rats up to the eighth day of pregnancy. All treatment groups, G3, and G4, showed significant weight loss at Pd4, whereas G1 showed weight gain postpartum. The mean body weights of the G1 had around 260 g. G2 had a slightly lower mean body weight of 245.7 g when compared to higher dose groups G3 and G4 showed lowest body weight of 242 and 240 g. The control group G1 gained weight, but the other groups lost significantly after Pd4. On Pd8, the treatment group had implantation issues in every case. In addition, a statistically significant difference in OBWR was found between groups, with the highest OBWR (p < 0.05) in G1 and the lowest in G4, as shown in Fig. 4(A). Meanwhile, it was found that UBWR was lower in G3 and G4 than in G2, whereas G1 had the greatest value (p < 0.05), as
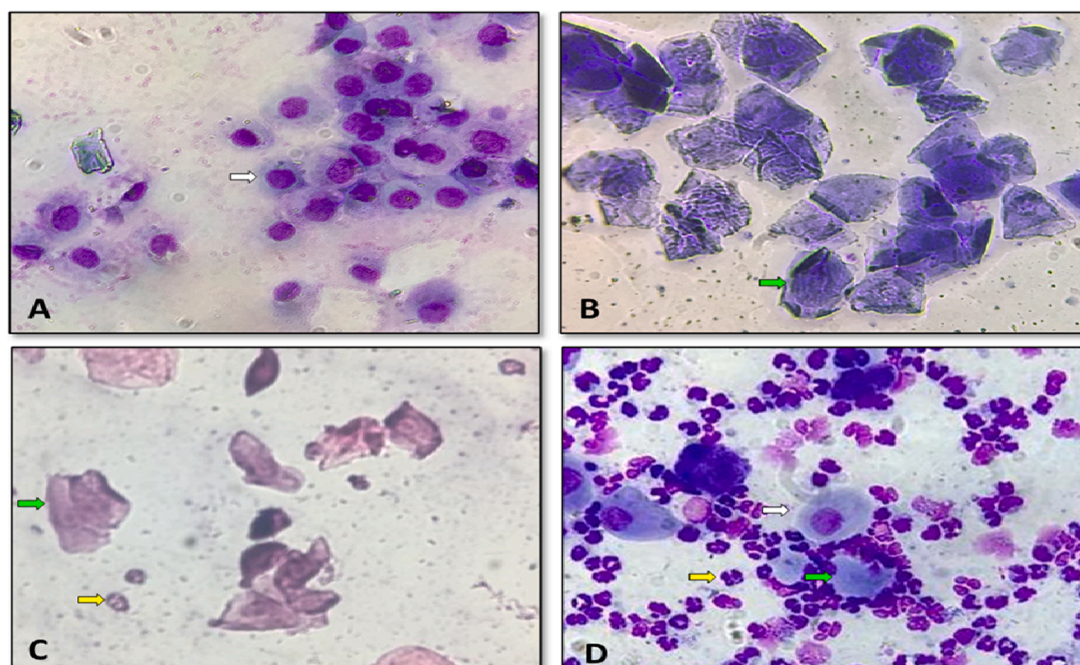
Fig. 1. Stages of the estrous cycle in SD rats monitored by the vaginal cytology. Where (A) Proestrus (B) Oestrus (C) Metoestrus (D) Dioestrus. Note: The white arrows represent the nucleated epithelial cells, the green for the cornified squamous epithelial cells, and the yellow arrows for the leukocytes: Giemsa stain, 400 × magnification.
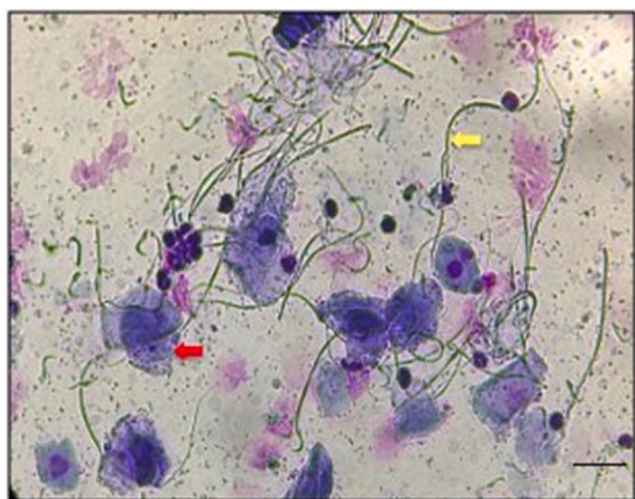
Fig. 2. Micrograph of the vaginal smear at Pd1. Here, the large number of sperms is represented by the yellow arrow, whereas the red arrows represent the cornified cells. Giemsa stain. 400 × magnification.

illustrated in Fig. 4(B).

3.3. Embryo implantation rate and fertility index

On the Pd8, the fertility index and the number of embryo implantation sites (EIS) were assessed to compare the control and treated groups. In Fig. 5, the sites appeared as tiny beads within G1 and G2. However, for groups G3 and G4, almost no implantation sites were visible. Thus, IMC treatment reduced implantation sites.

Fig. 6 shows the impact of IMC on EIS and the fertility index. While groups G1 and G2 had significantly higher EIS scores (A) and fertility index (B) than other groups; groups G3 and G4 dropped to zero.
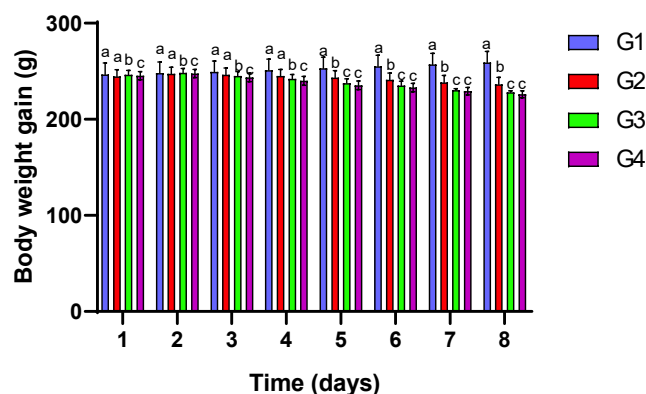
Fig. 3. Effects of IMC administration on body weight gain after pregnancy. Data are expressed as Mean ± SEM. Error bars showing different letters a, b, and c within rows denote a significant dif-ference at p < 0.05. *G1 = control, G2= (IMC 4.33 mg/kg bwt), G3= (IMC 4.66 mg/kg bwt), G4= (IMC 5.00 mg/kg bwt).

3.4. Effects of IMC on the development of follicles, corpora lutea and ovarian histomorphology

Fig. 7 shows the histopathological results of IMC on the ovaries of the examined groups. The ovaries had no noticeable pathological abnormalities. Regarding ovarian follicular dynamics, G3 and G4 had fewer surviving follicles (primary, secondary, and corpus lutea) than G1. As shown in Fig. 8, G4 had a higher proportion of atretic follicles than the other groups. As shown in Fig. 8, the IMC treatment groups had significant numbers of surviving follicles and corpus lutea. Fig. 9 shows vasoconstriction and inflammation in ovaries from all groups except G1. Mean scores of the histopathological lesions in the ovary show a significant infiltration of inflammatory cells in G2 and G3 (Table 2).
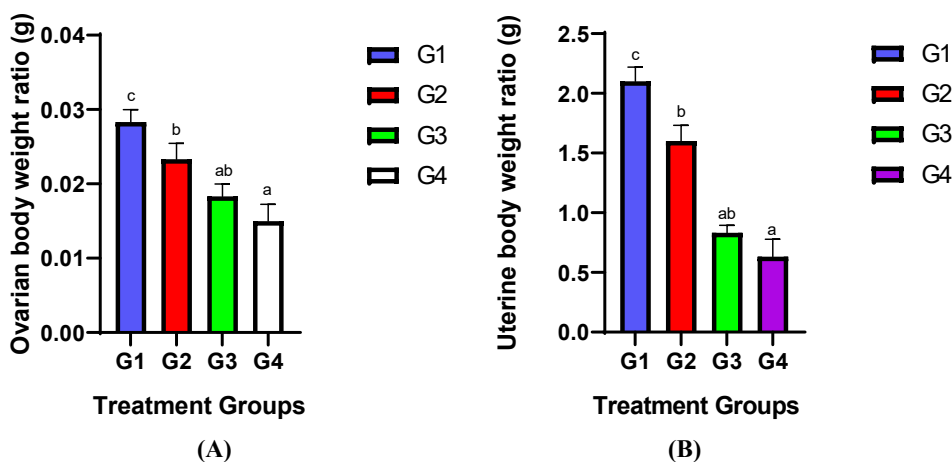
Fig. 4. Effect of IMC on OBWR (A) and UBWR (B). Data are expressed as Mean ± SE. Error bars with different letters a, b, and c within rows denote a significant difference at p < 0.05. *G1 = control, G2= (IMC 4.33 mg/kg bwt), G3= (IMC 4.66 mg/kg bwt), G4= (IMC 5.00 mg/kg bwt).
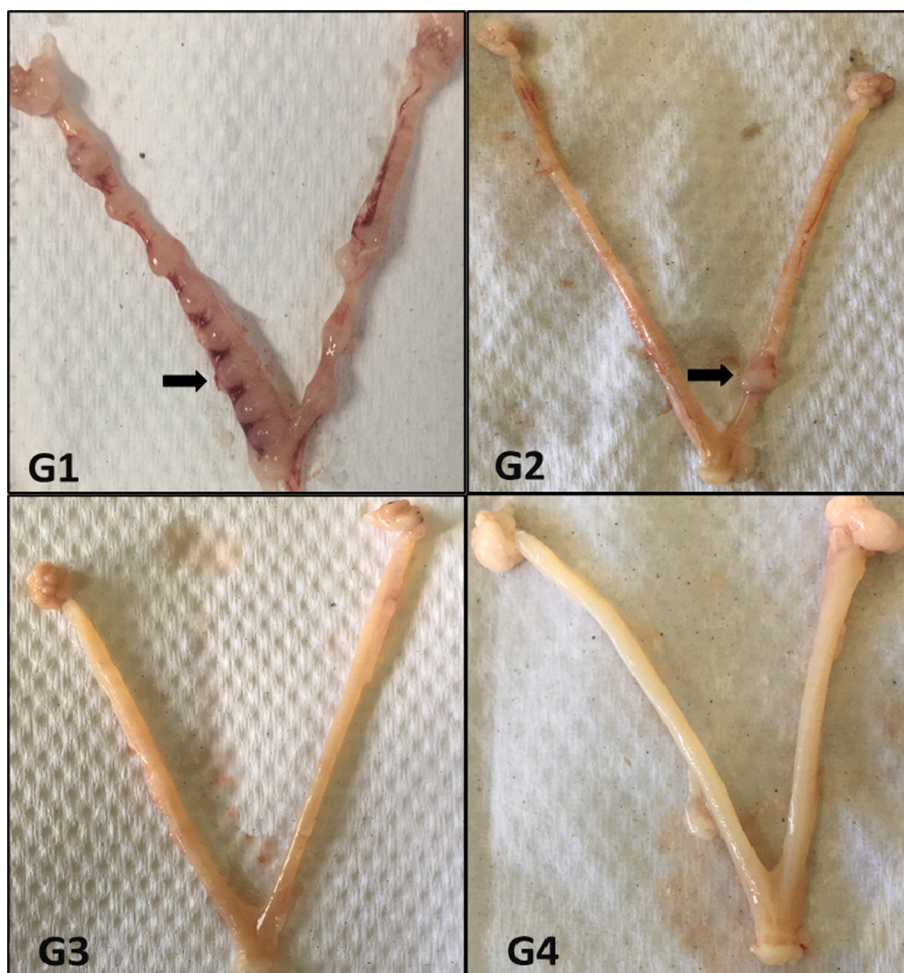
Fig. 5. Implanted embryo in the uteri of the rats (shown with a black arrow).

3.5. Uterine histomorphological analysis

No gross abnormalities were found in the uterus during this study. IMC caused pathological changes in the uteri of all three treatment groups. Except for G1, all other groups showed mild edema of the endometrium and detachment of the stromal cell of the endometrium from the uterine mucosa. Less endometrial glandular epithelium, smooth muscle cell layer atrophy and microvacuolation were found in G3 and G4, as shown in Fig. 10. Mean scores of histopathological lesions in the uterus show significant infiltration of inflammatory cells in G2, G3, and congestion in G2, G3, and G4 (Table 3).
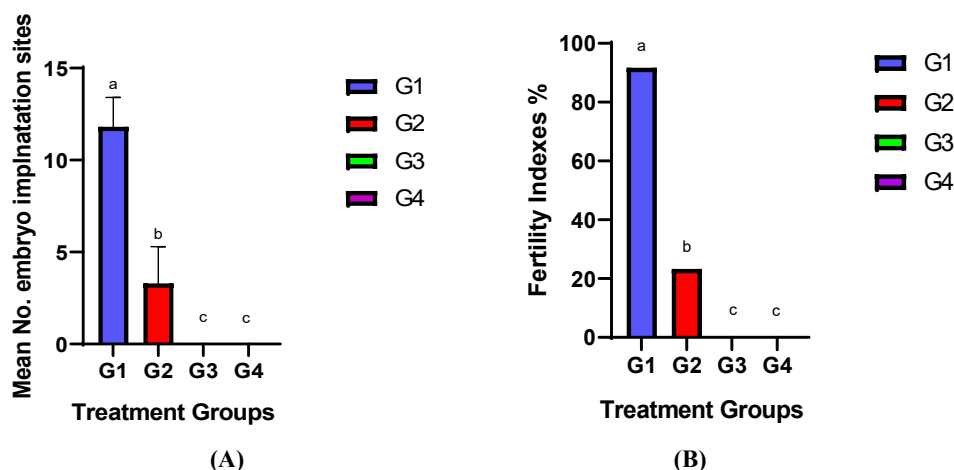
Fig. 6. Effects of IMC on EIS (A) and fertility index (B). Data are expressed as Mean ± SEM. Error bars with different letters a, b, and c denotes a significant difference at p < 0.05. Note, G1 = control, G2= (IMC 4.33 mg/kg bwt), G3= (IMC 4.66 mg/kg bwt), G3= (IMC 5.00 mg/kg bwt).
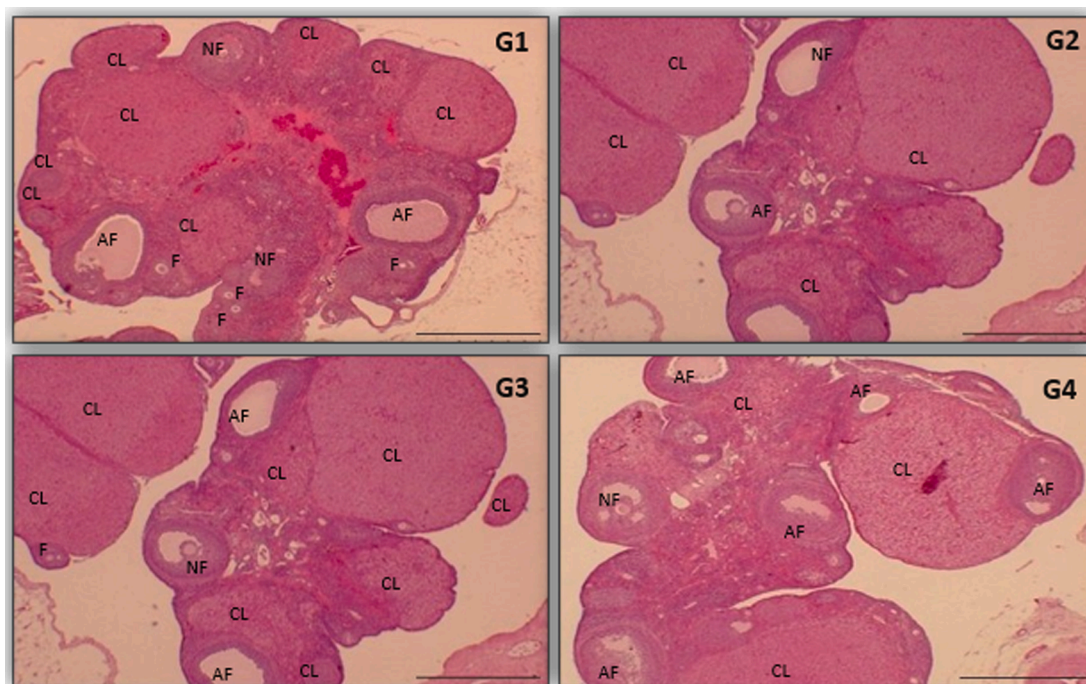
Fig. 7. Photomicrograph sections of control and IMC-exposed ovaries. Note: follicular unit = F; antral follicle = NF; atretic follicles = AF; corpus luteum = CL. H&E stain. Magnification 40×.

3.6. Kidney histomorphological analysis

Fig. 11 shows degenerative Bowman's capsule in SD rats administered doses of 4.66 and 5.00 mg/kg (groups G3 and G4). Compared to the treated groups, light microscopy revealed normal renal parenchymal structure in G1. The G3 renal tissues show significant necrosis as measured by the mean score of histopathologic lesions (Table 4).

3.7. Liver histomorphological analysis

As shown in Fig. 12, in group G4 microvacuolated hepatocytes, necrosis, and inflammatory cell infiltration were found while G2 and G3 exhibited hepatocyte vasoconstriction. Control group liver tissues had a typical normal structural organization, abundant binucleated hepatocytes, no inflammatory cell infiltration, and normal central veins (G1). In the histological sections of the livers of G2, G3, and G4, Kupffer cells

were found significantly activated (Table 5).

4. Discussion

Most NSAIDs have been reported to have an adverse effect on PG production by inhibiting the enzymatic activity of COX1 and COX2 (Ahmadi et al., 2022). In this study, SD rats received 4.33, 4.66 and 5.00 mg/kg bwt of IMC on Pd3 and Pd4, demonstrating maternal toxicity. These data are consistent with the findings of a previous study (Damasceno et al., 2008) which demonstrated a decrease in feed intake and body weight from Pd6 to Pd11 in SD rats administered an IMC dose of 8.50 mg/kg bwt. In addition, IMC treatment has an adverse effect on the smooth muscles of the small intestine and a reduced number of embryos were observed. This dramatically reduces the length of the small intestine and number of EIS (Menozzi et al., 2011). IMC, a COX-inhibiting NSAID, has also been shown to reduce EIS (Ikeda et al., 2019).
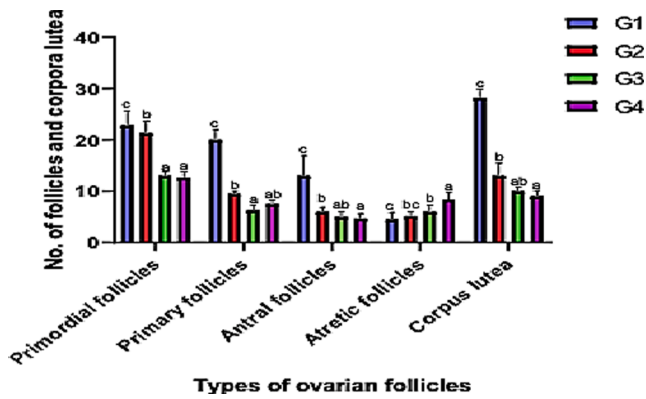
Fig. 8. Effect of IMC on follicular development after female rats were exposed to IMC. Data are expressed as M ± SEM. Error bars show different letters a, b, and c denotes a significant difference at $p < 0.05$. *G1 = control, G2= (IMC 4.33 mg/kg bwt), G3= (IMC 4.66 mg/kg bwt), G4= (IMC 5.00 mg/kg bwt).

In the current study a significant drop in EIS was observed in IMC doses 4.66 and 5.00 mg/kg bwt were observed when compared to control group. Furthermore, the toxic dam-age to uterine tissues caused by IMC may contribute to the loss of implantations in the treated groups by impairing the ability of endometrial cells to produce PG (Damasceno et al., 2008). The effect of IMC has been attributed to its ability to inhibit PG synthesis in the uterus (Bergström, 2014). Further-more, inhibition of COX-2 results in a restrictive response to blastocyst implantation, while simultaneous inhibition of COX-1 and COX-2 isoforms due to IMC supplements results in more significant adverse effects on implantation (Sookvanichsilp & Pulbutr, 2002). Numerous miscarriages, including defects in ovulation, implantation, and fertilization, have been directly linked to female COX-2 deficiency (Song et al., 2000). Another study revealed uterine smooth muscle atrophy and vasoconstriction following IMC treatment, resulting in decreased uterine smooth muscle

contraction and uterine glands (Mohan & Bennett, 2006).

Most of the research published to date has focused on the adverse effects of IMC on the re-productive health of Wistar rats. However, there is less research on the effectiveness of IMC treatment in establishing EID in SD rats. When IMC was administered at a dose of 5 mg/kg on Pd3 and Pd4 and 10 mg/kg/day on Pd1 to Pd7, the number of embryo implantation sites was reduced (Sookvanichsilp & Pulbutr, 2002). But when IMC was administered subcutaneously at a dose of 1 mg/kg twice on Pd5, no significant changes in the number of implantation sites were found (Kennedy, 1977). In this case, using IMC on Pd5 instead of Pd3 can be blamed for the reduced effectiveness of IMC.

The number of EIS was reduced in studies with IMC doses of 3 and 5 mg/kg bwt administered twice daily from Pd3 to Pd5 (Phillips & Poyser, 1981). Toxic gastrointestinal hemorrhage and fatalities have been reported at 8.40 mg/kg/day and 10 mg/kg/day (Damasceno et al., 2008; Salleh, 2014; Shafiq et al., 2004). In another study, Both pre-and post-implantation losses increased significantly at a dose of 10 mg/kg/day (Shafiq et al., 2004). The reproductive health of Wister rats was not affected at lower doses of 0.32, 1, and 1.68 mg/kg bwt twice daily from Pd3 to Pd5 (Damasceno et al., 2008; Kennedy, 1977). EIS was significantly reduced in all rat groups treated with IMC in the current study. The 4.33 mg/kg dose resulted in a low number of EIS, although the liver and kidney were not adversely affected to a significant extent. Vaso-constriction and vascularization in uterine tissues have been observed as side effects of the treatment of IMC. According to the findings of this study, the restriction of PGs by the IMC is believed to be the cause of vasoconstriction in uterine tissues (Ekanem et al., 2008). Aside from ischemia, smooth muscle atrophy can directly result from a loss of blood flow to the muscle (Bishop-Bailey & Warner, 2003). Thus, it can be stated that in sufficient doses, IMC can establish EID. Lethargy, abdominal edema, and decreased appetite were observed throughout this study as indicators of IMC-induced toxicity (Kaplan et al., 2012).

Nevertheless, the results of this study show that the IMC doses caused by PG inhibition leads to reducing uterine hypercontractility, pressure, ischemia, and pain, which is hazardous. High doses of NSAID have been
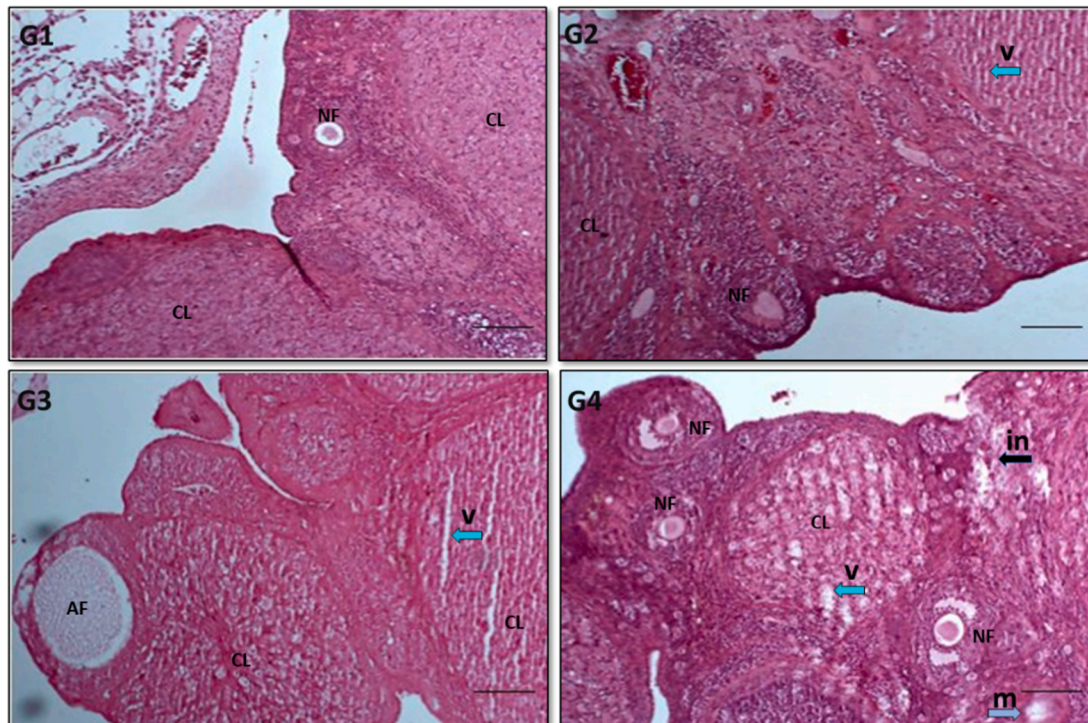
Fig. 9. Histopathological analysis of the ovaries. Note: follicular unit = F; antral follicle = NF; atretic follicles = AF; corpus luteum = CL. H&E stain. Here, a micrograph of the ovaries of the control group (G1) compared to the treated groups (G2, G3, and G4), showing areas of vasocon-striction (v) with a blue arrow, inflammatory changes (in) with a black arrow and smooth muscle atrophy (m), with a grey arrow. Magnification 400×.
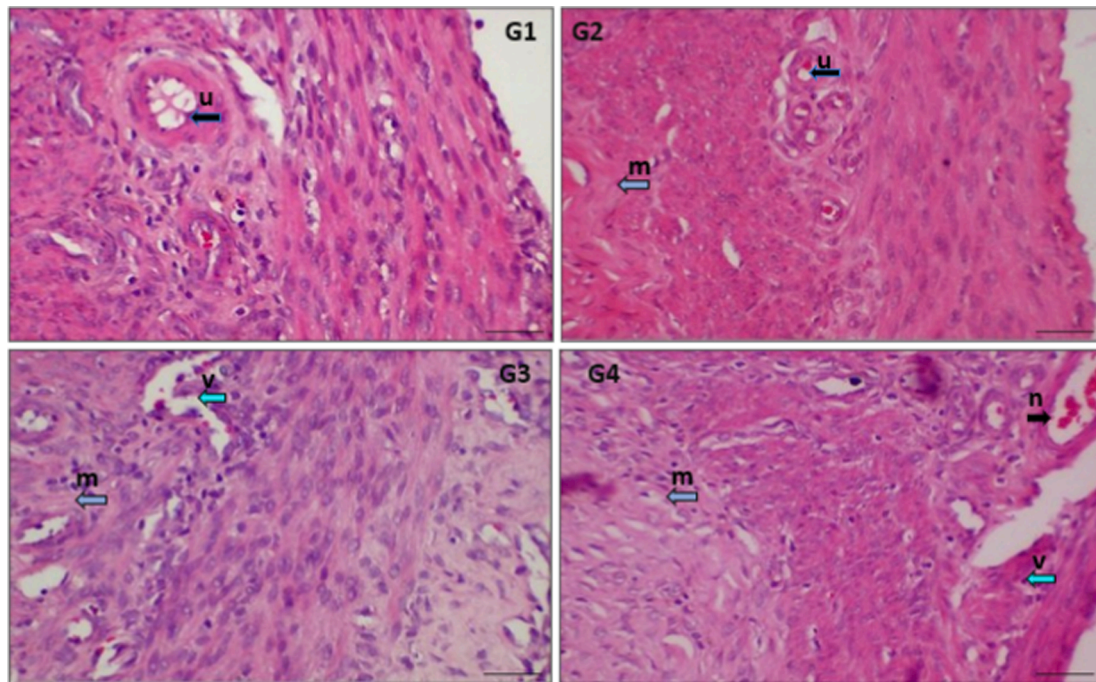
Fig. 10. Uterine histopathological analysis. H&E stain. Here, the micrograph of the uterus of the rat of the control group (G1) compared to the treated groups (G2, G3, G4) shows the areas of vasoconstriction (v), indicated with a blue arrow, blood vessels (b), with a green arrow and smooth muscle atrophy (m) with a grey arrow and the uterine gland (u) indicated by the black arrow. Magnification 400×.
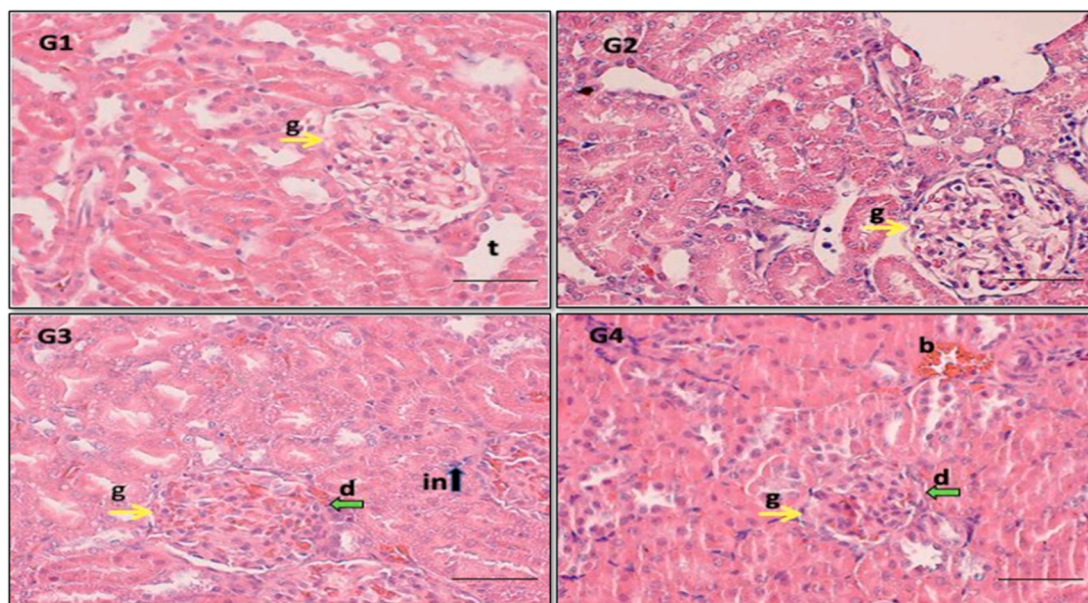
Fig. 11. Micrograph of the kidney. Here, the micrograph of the control group (G1) kidney shows the normal histological structure of renal parenchyma compared to treatment groups (G2, G3, G4), showing congestion of intertubular blood vessels (b), distal tubules (t), degenerative Bowmen's capsule (d), with a green arrow, inflammatory cells (in), distal tubules (t), and glomerulus (g) shown with a yellow arrow. H&E stain. Magnification 400×.

shown to alter the walls of the uterine horns and decrease the capacity of the lumen and the layers of the lamina propria and the epitheli-um (Güven et al., 2013). Similarly, the treatment of IMC drastically reduced the uterine horn and ancillary functions, as well as ciliary activity and the uterine horns lumen. According to previous study from renal excision, increased renal PG excretion is the leading cause of elevated COX-2 expression (Sanchez et al., 1999). Vasoconstriction, dilatation, and congestion of intertubular blood vessels, as well as a degenerative Bowman's capsule, were histopathologically detected in

the present study.

On the other hand, IMC reliably blocked the ovulation of preovulatory follicles at low doses, leading to ovarian cyst development (Tokmakov et al., 2020; Vernunft et al., 2022). In an experiment conducted by (Orczyk, 1972) at a single dose of 7 mg/kg if IMC administered (SC) showed complete inhibition of ovulation when observed at 3.5 h prior to the expected ovulatory LH surge, while all rats were reported to ovulate after LH was administered 3 h after a dose of 1 mg/kg of IMC (Orczyk & Behrman, 1972). In another study those female mice that received 7.5
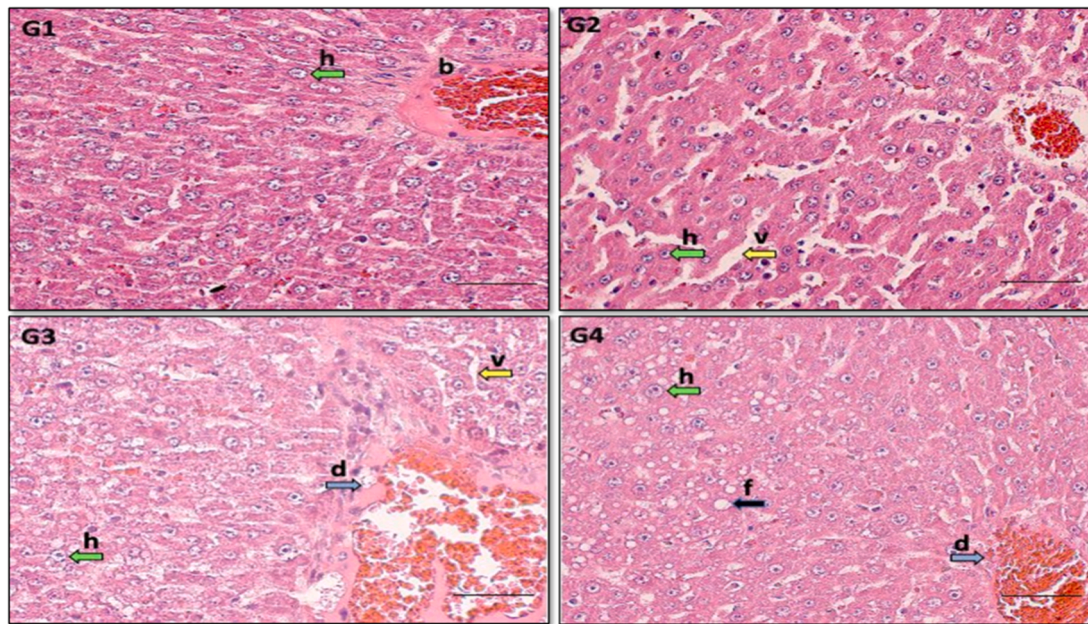
Fig. 12. Micrograph of the liver sections of rats subjected to different doses of IMC. Here is a micrograph of the liver of the control group (G1) compared to the treatment groups (G2, G3, G4). Hepatocytes are shown with a green arrow, blood vessel (b), vascularization (f) with a black arrow, vasoconstriction (v) with a yellow arrow, hepatocytes (h) with a green arrow, and the apoptotic degeneration of cells (d) are shown with a blue arrow. H&E stain, Magnification 400×.

mg/kg NSAIDs, showed enlarged, congested ovaries with cystic appearance and congested uteri with prominent blood vessels (Al-Atrakji et al., 2012). In the current study rat ovaries treated with higher doses (4.66 and 5 mg/kg) of IMC were observed with congestion and inflammatory changes.

In contrast to these pathological findings, the treated SD rats in G2 showed no changes to their kidneys other than microvacuoles in their epithelial linings. Progesterone levels and corpora luteum counts increased in G1 compared to the other groups, indicating that cor-pora luteum counts were also increasing. According to a previous study, vasoconstriction of parts of the ovaries indicated blocked blood arteries. There were no noticeable clinical or histological gross abnormalities in the ovaries of rats treated with vasoconstriction (Niebyl et al., 1980). Microvacuolation of hepatocytes was confirmed in histological studies at 5.00 mg/kg and 8.40 mg/kg IMC. Rats in G4 also developed ulcers in their colons. The results of this study were in complete agreement with those found in (Salleh, 2014; Sookvanichsilp & Pulbutr, 2002). As a result, by analyzing the EIS and histomorphological changes in the ovaries, uterus, kidney, and liver of SD rats in the current study, it can be concluded that IMC harms the reproductive health of SD rats at a dose of 4.33 mg/kg bwt or greater.

5. Conclusion

To our knowledge this is the first study to evaluate the effect of IMC in disrupting EID in SD rats whereby a dosage of 4.33 mg/kg bwt given twice on Pd3 and Pd4, is effective enough to establish EID model rats without severely affecting other vital organs of the body. The IMC treatment disrupted the implantation process, caused a significant reduction in embryo development, and showed signs of vasoconstriction and uterine smooth muscle atrophy. Assessment of the EIS and histo-morphological changes in the ovaries, uterus, kidneys, and liver of SD rats in a laboratory experiment revealed vasoconstriction and showed endometrial atrophy and vasocontstrction in uterus, a destructive Bowmen's capsule was observed in the kidneys and microvacuolation of hepatocytes in the liver.

Declaration of competing interest

The authors declare that they have no known competing financial interests or personal relationships that could have appeared to influence the work reported in this paper.

References

Ahmadi, M., Bekeschus, S., Weltmann, K.-D., von Woedtke, T., Wende, K., 2022. Non-steroidal anti-inflammatory drugs: recent advances in the use of synthetic COX-2 inhibitors. RSC Med. Chem. 13 (5), 471–496.

Al-Atrakji, M.Q., Al-Zohyri, A.M., Al-Janabi, A.S., 2012. Comparative study of the effects of some NSAIDs on ovulation in female mice. J. Faculty Medicine Baghdad 54 (2), 158–162.

Albishtue, A.A., Yimer, N., Zakaria, M.Z.A., Haron, A.W., Yusoff, R., Almhanawi, B.H., 2018. Ameliorating effect of edible Bird's Nest against lead acetate toxicity on the rat hypothalamic–pituitary–ovarian axis and expressions of epidermal growth factor and vascular endothelial growth factor in ovaries. Comparative Clin. Pathol. 27 (5), 1257–1267.

Andrabi, S., Maxwell, W., 2007. A review on reproductive biotechnologies for conservation of endangered mammalian species. Anim. Reprod. Sci. 99 (3–4), 223–243.

Bergström, S., 2014. Advances in the Biosciences: International Conference on Prostaglandins, Vienna, September 25 to 28, 1972, Elsevier.

Bishop-Bailey, D., Warner, T.D., 2003. PPARγ ligands induce prostaglandin production in vascular smooth muscle cells: indomethacin acts as a peroxisome proliferator-activated receptor-γ antagonist. FASEB J. 17 (13), 1–15.

Cavalieri, J., Kinder, J., Fitzpatrick, L., 1998. Duration of ovulation suppression with subcutaneous silicone implants containing norgestomet in Bos indicus heifers and cows. Anim. Reprod. Sci. 51 (1), 15–22.

Damasceno, D.C., Volpato, G.T., Ferrari, C., Roldan, L.B., Souza, M.d.S.S., 2008. Effect of indomethacin on the pregnant rat. Braz. Arch. Biol. Technol. 51, 75–81.

Duncan, W. C. (2019). Physiology of Ovulation. How to Prepare the Egg and Embryo to Maximize IVF Success. In: Kovacs, G., Rutherford, A., Gardne, D.K. (Eds.), pp. 1-21.

Ekanem, A., Garba, S., Jankada, A., 2008. Histomorphological assessments of the female reproductive organs of rats under indomethacin and aspirin treatments. J. Pharmacol. Toxicol. 3 (3), 203–212.

Fu, C., Mao, W., Gao, R., Deng, Y., Gao, L., Wu, J., Zhang, S., Shen, Y., Liu, K., Li, Q., 2020. Prostaglandin F2α-PTGFR signaling promotes proliferation of endometrial epithelial cells of cattle through cell cycle regulation. Anim. Reprod. Sci. 213, 106276.

Güven, D., Altunkaynak, B., Ayranci, E., Kaplan, S., Bildircin, F., Kesim, Y., Rağbetli, M., 2013. Stereological and histopathological evaluation of ovary and uterine horns of female rats prenatally exposed to diclofenac sodium. J. Obstet. Gynaecol. 33 (3), 258–263.

Ikeda, A., Funakoshi, E., Araki, M., Ma, B., Karuo, Y., Tarui, A., Sato, K., Okuno, Y., Kawai, K., Omote, M., 2019. Structural modification of indomethacin toward selective inhibition of COX-2 with a significant increase in van der Waals contributions. Bioorg. Med. Chem. 27 (9), 1789–1794.

Kaplan, K.A., Odabasoglu, F., Halici, Z., Halici, M., Cadirci, E., Atalay, F., Aydin, O., Cakir, A., 2012. Alpha-lipoic acid protects against indomethacin-induced gastric oxidative toxicity by modulating antioxidant system. J. Food Sci. 77 (11), H224–H230.

Kennedy, T., 1977. Evidence for a role for prostaglandins in the initiation of blastocyst implantation in the rat. Biol. Reprod. 16 (3), 286–291.

Khan, S., Yusufi, F.N.K., Yusufi, A.N.K., 2019. Comparative effect of indomethacin (IndoM) on the enzymes of carbohydrate metabolism, brush border membrane and oxidative stress in the kidney, small intestine and liver of rats. Toxicol. Rep. 6, 389–394.

Lü, Z., Zhu, K., Pang, Z., Liu, L., Jiang, L., Liu, B., Shi, H., Ping, H., Chi, C., Gong, L., 2019. Identification, Characterization and mRNA Transcript Abundance Profiles of Estrogen Related Receptor (ERR) in Sepiella Japonica Imply Its Possible Involvement in Female Reproduction. Animal Reproduct. Sci. 211, 106231.

Mahmoud, M.F., Abdo, W., Nabil, M., Drissi, B., El-Shazly, A.M., Abdelfattah, M.A., Sobeh, M., 2023. Apple (Malus domestica Borkh) leaves attenuate indomethacin-induced gastric ulcer in rats. Biomed. Pharmacother. 160, 114331.

Menozzi, A., Pozzoli, C., Poli, E., Passeri, B., Gianelli, P., Bertini, S., 2011. Diazoxide attenuates indomethacin-induced small intestinal damage in the rat. Eur. J. Pharmacol. 650 (1), 378–383.

Mohan, A.R., Bennett, P.R., 2006. Drugs acting on the pregnant uterus. Curr. Obstet. Gynaecol. 16 (3), 174–180.

Niebyl, J.R., Blake, D.A., White, R.D., Kumor, K.M., Dubin, N.H., Robinson, J.C., Egner, P.G., 1980. The inhibition of premature labor with indomethacin. Am. J. Obstet. Gynecol. 136 (8), 1014–1019.

Olivera-Muzante, J., Fierro, S., Alabart, J., Minteguiaga, M., Aunchayna, G., Errandonea, N., Banchero, G., 2019. Short-term dietary protein supplementation improves reproductive performance of estrous-synchronized ewes when there are long intervals of prostaglandin or progesterone-based treatments for timed AI. Anim. Reprod. Sci. 206, 78–84.

Orczyk, G.P., Behrman, H.R., 1972. Ovulation blockade by aspirin or indomethacin-in vivo evidence for a role of prostaglandin in gonadotrophin secretion. Prostaglandins 1 (1), 3–20.

Pallares, P., Gonzalez-Bulnes, A., 2009. A new method for induction and synchronization of oestrus and fertile ovulations in mice by using exogenous hormones. Lab. Anim 43 (3), 295–299.

Parthasarathy, M., Evan Prince, S., 2021. The potential effect of phytochemicals and herbal plant remedies for treating drug-induced hepatotoxicity: a review. Mol. Biol. Rep. 48, 4767–4788.

Phillips, C.A., Poyser, N., 1981. Studies on the involvement of prostaglandins in implantation in the rat. Reproduction 62 (1), 73–81.

Poyser, N., 1999. A comparison of the effects of indomethacin and NS-398 (a selective prostaglandin H synthase-2 inhibitor) on implantation in the rat. Prostaglandins, Leukotrienes and Essential Fatty Acids (PLEFA) 61 (5), 297–301.

Salleh, N., 2014. Diverse roles of prostaglandins in blastocyst implantation. Scientific World J.

Sanchez, P.L., Salgado, L.M., Ferreri, N.R., Escalante, B., 1999. Effect of cyclooxygenase-2 inhibition on renal function after renal ablation. Hypertension 34 (4), 848–853.

Sathyanarayanan, S., Sreeja, P.S., Arunachalam, K., Parimelazhagan, T., 2022. Toxicity and antiulcer properties of *Ipomoea wightii* (Wall.) choisy leaves: an in vivo approach using wistar albino rats. Evidence-Based Complement. Alternative Med.

Shafiq, N., Malhotra, S., Pandhi, P., 2004. Comparison of nonselective cyclo-oxygenase (COX) inhibitor and selective COX-2 inhibitors on preimplantation loss, postimplantation loss and duration of gestation: an experimental study. Contraception 69 (1), 71–75.

Song, H., Lim, H., Das, S.K., Paria, B.C., Dey, S.K., 2000. Dysregulation of EGF family of growth factors and COX-2 in the uterus during the preattachment and attachment reactions of the blastocyst with the luminal epithelium correlates with implantation failure in LIF-deficient mice. Mol. Endocrinol. 14 (8), 1147–1161.

Sookvanichsilp, N., Pulbutr, P., 2002. Anti-implantation effects of indomethacin and celecoxib in rats. Contraception 65 (5), 373–378.

Steenbergen, P.J., Heigwer, J., Pandey, G., Tönshoff, B., Gehrig, J., Westhoff, J.H., 2020. A multiparametric assay platform for simultaneous in vivo assessment of pronephric morphology, renal function and heart rate in larval zebrafish. Cells 9 (5), 1269.

Thompson, R.P., Nilsson, E., Skinner, M.K., 2020. Environmental epigenetics and epigenetic inheritance in domestic farm animals. Anim. Reprod. Sci. 220, 106316.

Tokmakov, A.A., Stefanov, V.E., Sato, K.-I., 2020. Dissection of the ovulatory process using ex vivo approaches. Front. Cell Dev. Biol. 8, 605379.

Tranguch, S., Daikoku, T., Guo, Y., Wang, H., Dey, S., 2005. Molecular complexity in establishing uterine receptivity and implantation. Cell. Mol. Life Sci. 62, 1964–1973.

Vernunft, A., Lapp, R., Viergutz, T., Weitzel, J.M., 2022. Effects of different cyclooxygenase inhibitors on prostaglandin E2 production, steroidogenesis and ovulation of bovine preovulatory follicles. J. Reprod. Dev. 68 (4), 246–253.

Yavuz, A., Oner, G., Tas, M., Sonmezer, M., 2021. The impact of indomethacin on the number of oocytes retrieved and IVF outcomes in patients with poor ovarian response. Eur. J. Obstetrics Gynecol. Reproductive Biol. 264, 266–270.

Yerushalmi, G.M., Shuraki, B., Yung, Y., Maman, E., Baum, M., Hennebold, J.D., Adashi, E.Y., Hourvitz, A., 2023. ABCC4 is a PGE2 efflux transporter in the ovarian follicle: a mediator of ovulation and a potential non-hormonal contraceptive target. FASEB J. 37 (4), e22858.